Biophysical Journal Volume 70 February 1996 962–970

Chromophore Reorientations in the Early Photolysis Intermediates of Bacteriorhodopsin

Raymond M. Esquerra, Diping Che, Daniel B. Shapiro, James W. Lewis, Roberto A. Bogomolni,
Jorge Fukushima, and David S. Kliger
Department of Chemistry and Biochemistry, University of California at Santa Cruz, Santa Cruz, California 95064 USA

ABSTRACT The photoselection-induced time-resolved linear dichroism of a bacteriorhodopsin suspension of purple membrane from 350 to 750 nm is measured by a new pseudo-null measurement technique. In combination with time-resolved absorption measurements, these linear dichroism measurements are used to determine the reorientation of the retinal chromophore of bacteriorhodopsin from 50 ns to 50 μs after photolysis. This time range covers the times when the K photointermediate decays to form L, as well as the early times during the formation of the M intermediate in the photocycle. An analysis of the photoselection-induced linear dichroism measured directly, along with the absorbance changes polarized parallel to the linearly polarized excitation, shows that the anisotropy is invariant over this time period, implying that the photolyzed chromophore rotates less than 8°C with respect to unphotolyzed chromophores during this part of the photocycle.

INTRODUCTION

Bacteriorhodopsin (bR) is the membrane-bound protein of the purple membrane (PM) of *Halobacterium salinarium* (formerly referred to as *Halobacterium halobium*). The PM is made of bR trimers that are arranged in a two-dimensional hexagonal lattice (Henderson, 1975). Light-adapted bR contains the linear chromophore all-*trans* retinal, covalently bound to the protein through a protonated Schiff base linkage. The absorption of light by the chromophore induces a reversible isomerization, which initiates a series of protein conformational changes that serves to pump protons across the membrane (Stoeckenius et al., 1979). This functions as a light energy to chemical energy transduction mechanism by which *H. salinarium* can survive. Several spectral intermediates, labeled J, K, L, M, N, and O, have been identified with lifetimes ranging from femtoseconds to milliseconds (for recent reviews see Mathies et al., 1991; Lanyi, 1992; and Birge, 1990). These intermediates undergo a photocycle that regenerates bR as schematically diagrammed in Fig. 1 (Lozier et al., 1975), although more-complex models have been presented (Lanyi, 1992).

The ability of bR to use light energy to pump protons across a membrane makes it a useful model for the function and structure of a large family of related proteins. Bacteriorhodopsin is a seven-helix trans-membrane protein similar to many sensory protein systems, such as rhodopsin and the muscarinic acetylcholine receptor. Inasmuch as the isomerization of the bR chromophore induces the conformational changes that enable proton pumping to occur, it is desirable to determine the degree of reorientation of the chromophore over the course of the photocycle to determine any role that this motion plays in the mechanism of proton pumping. Because the all-*trans* and the 13-*cis* chromophores are essentially linear, the orientation of the transition dipole moment is a good indication of the chromophore's orientation. Thus, linear dichroism should provide information about the relationship between chromophore motion and the proton pumping mechanism.

A great deal is known about the later photolysis intermediates because the M intermediate can be stabilized by mutation and by environmental conditions, such as pH, allowing detailed structural study of the protein in the M intermediate with respect to the ground-state bR. Electron diffraction (Subramaniam et al., 1993; Han et al., 1994), neutron diffraction (Dencher et al., 1989), and x-ray diffraction (Koch et al., 1991) studies concur that there are protein conformational changes between the ground-state bR and the M intermediate. These studies, however, do not deal specifically with the chromophore. A recent neutron diffraction study on deuterated retinals (Hauss et al., 1994) that focused on the chromophore indicated that the C-5 to C-13 part of the polyene chain of the chromophore changes its out-of-plane tilt toward the cytoplasm by 11° ± 6° between the ground-state bR and the M intermediate. The M intermediate multilayer sample was prepared by exposure to 0.1- or 1-M guanidine hydrochloride and rapidly cooled to 90 K after illumination. These motions were also studied by transient linear dichroism measurements on oriented immobilized PM of bR and the M intermediate (Heyn and Otto, 1992), which place a lower bound on the motion of the polyene backbone. The transient linear dichroism measurements on immobilized samples in gel by Heyn and Otto (1992) detect no changes greater than 3° between the transition dipole moments of bR and the M intermediate. A recent linear dichroism study of immobilized samples shows that the transition dipole moment for the O intermediate rotates less than 4° with respect to that of unphoto-

---

Received for publication 11 July 1995 and in final form 15 November 1995.

Address reprint requests to Dr. David S. Kliger, Department of Chemistry and Biochemistry, University of California at Santa Cruz, Santa Cruz, CA 95064. Tel.: 408-459-2106; Fax: 408-459-2935; E-mail: kliger@chemistry.ucsc.edu.

0006-3495/96/02/962/09 $2.00

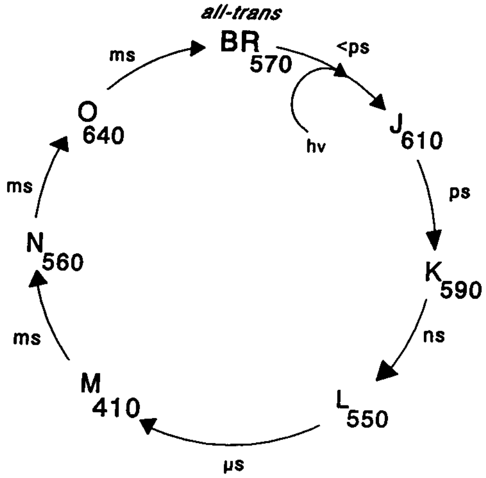

FIGURE 1 Photocycle of bR. Intermediates are shown with their spectral absorbance maxima and approximate lifetimes.

lyzed bR (Otto et al., 1995). Also, a recent ^{2}H-NMR result on the M intermediate in oriented, hydrated membrane films shows that the orientation of the C_{19} methyl group changes by only 4° (Ulrich et al., 1995). However, because these studies were not done with aqueous PM suspensions, it is possible that the chromophore in PM behaves differently in suspensions

Some transient linear dichroism studies on PM suspensions (Lozier and Bogomolni, unpublished results) and on PM in oriented molecular films (Hwang et al., 1977) measure no significant changes in the orientation of the transition dipole moment over the course of the photocycle. However, transient linear dichroism studies by Ahl and Cone (1984) with 1-ms resolution on aqueous membranes suggested that there is a rotation of the chromophore with respect to the unphotolyzed bR larger than 10°. In combination with linear dichroism studies of glutaraldehyde fixed membranes, in which this rotation decreased below the 5° sensitivity limit of the experiment, they attributed the large observed rotation to differential protein rotation of the two nonexcited chromophores of the trimers, which are sometimes called "spectators," with respect to the cycling protein (and not chromophore rotations within the protein). These results are supported by the results of Wan et al. (1993), obtained with better time resolution. Czégé and Reinisch (1990) have observed large-scale light-scattering changes with microsecond resolution that they associate with curvature changes of the membrane patch during the course of the photocycle. These results suggest that there are possibly large changes of protein orientations in the patch that might be observed by monitoring the linear dichroism of the chromophore. Some early-time anisotropy studies (Wan et al., 1990) and some linear dichroism studies (Wan et al., 1991) of the early K and L intermediates suggest that the transition dipole moment may rotate as much as 20° during the K to L transition. Song et al. (1994), measuring linear dichroism changes in aqueous suspensions, have seen substantial reorientations of the transition dipole moment, as much as 8° for the K intermediate and as much as 20° for the M intermediate. These changes are larger than expected from the structural studies of the protein or from the linear dichroism studies of immobilized gel samples of bR in the M and the O intermediates. It is important to reconcile the different results for immobilized samples (in which the measurements should be more sensitive), for which small reorientations are observed, with measurements on PM suspensions, for which large reorientations are observed in some (but not all) studies.

Historically, linear dichroism studies of aqueous PM are complicated by the depolarization effects of rotational diffusion of membrane patches and the limits of sensitivity in the region where the linear dichroism (LD) signal is linear with respect to photolysis. Avoiding saturation requires photolysis of much less than 5%, which leads to LD photolysis signals of less than 0.05 optical density unit for samples with a ground-state absorbance of ~1. Typically, only single-wavelength LD studies have been presented, where the benefits of laser light sources and modulation techniques can be applied.

Here we apply a new sensitive method to measure transient time-resolved LD to the bR phototransformations from the K to the early M intermediate across the entire spectral region of 350–750 nm. In combination with transient absorption spectroscopy of the K through M transitions, we determine that the chromophore rotates less than 8°.

THEORY OF THE TECHNIQUE

Ultrasensitive time-resolved linear dichroism measurements

The pseudo-null time-resolved LD method was previously described in detail (Che et al., 1994b). Its optical layout is depicted in Fig. 2. It consists of a sample placed between two crossed polarizers. One makes a LD measurement by rotating the first polarizer clockwise, as viewed looking

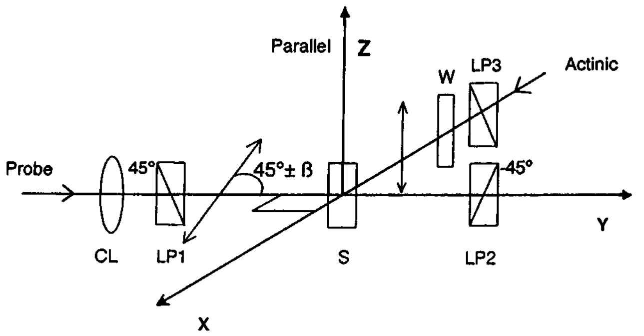

FIGURE 2 Optical apparatus: *Probe*, flash-lamp probe source; *CL*, collimating lens; *LP1*, *LP2*, Glan–Taylor polarizers set at 45° and -45°, respectively, with respect to the *z* axis; *S*, sample; *LP3*, excitation Glan–Taylor laser polarizer set exactly parallel to the *z* axis; *W*, half-wave plate; *Actinic*, excitation laser pulse, which is linearly polarized along the *z* axis; β, small rotation angle.

toward the detector, and then counterclockwise by a small angle, β, from the crossed position. The measured signal is the ratio of the difference to the sum of the clockwise and counterclockwise positions,

$$\text{signal}(t) = \frac{I_+(t) - I_-(t)}{I_+(t) + I_-(t)}, \tag{1}$$

where + and - symbolize clockwise and counterclockwise rotations, respectively. For samples for which the contribution of circular birefringence (CB) is negligible compared with the LD, as is the case with photoselected bR, the measured signal after photoselection with a linearly polarized excitation beam becomes (Che et al., 1994b)

$$\text{signal}\ (t) = \frac{\text{LD}(t)}{\beta} = \frac{(\Delta A_{\parallel}(t) - \Delta A_{\perp}(t))}{\beta}, \tag{2}$$

where LD(t) is the time-dependent linear dichroism and $\Delta A_{\parallel}(t)$ and $\Delta A_{\perp}(t)$ are the time-dependent absorption difference between the absorption of photointermediates at a time t after the excitation pulse and the sample before excitation, for the probe beam polarized parallel and perpendicular to the linearly polarized excitation beam, respectively. The phototransformation of the selected bR molecules was monitored at different times following the actinic pulse by use of a gated detector.

With β (in radians) less than 1, there is a magnification of the LD signal. Therefore, with the same transmitted intensity, this pseudo-null technique gives a larger ratio between LD and transmitted intensity and thus yields a much better signal-to-noise ratio than the standard method that modulates the polarization states of the probe beam by ±90°.

Determination of orientational dynamics

This method for time-resolved LD can increase the signal-to-noise ratio as much as a hundredfold, and this makes broadband spectral measurements more feasible. However, because LD is a function of both sample absorption and the orientation of transition dipole moments, LD alone does not fully determine the orientational dynamics of transition dipole moments. Additional information, such as any combination of parallel or perpendicular absorption, is also required for a complete determination of the anisotropy. From a signal-to-noise ratio consideration, if the angle between the transition dipole moments is smaller than the magic angle, 54.7°, it is advantageous to measure the parallel absorption difference, $\Delta A_{\parallel}(t)$, rather than to measure both $\Delta A_{\parallel}(t)$ and $\Delta A_{\perp}(t)$ independently. This was the approach that we used to obtain the data presented here. The combination of the ultrasensitive LD technique and the measurement of the parallel absorption gives an increase in the anisotropy signal-to-noise ratio close to a factor of 3 if small reorientations of the transition dipole moment are involved.

MATERIALS AND METHODS

Samples of bR (from the strain ET-1001) were prepared by established procedures (Oesterhelt and Stoeckenius, 1971). The PM was suspended in 2-mM HEPES (Sigma) and 4-mM NaCl at pH 6.9. We sonicated the sample for 7 s to reduce the average size of the PM patches (see Results and Discussion), using the 2-mm tip of a Microson Ultrasonic Cell Distrupter (Heat Systems Ultrasonics, Inc., Farmingdale, NY) set at 20. The sample was light adapted by irradiation with a tungsten lamp (Cole Palmer Instrument, Chicago, IL, Model 9741–50) in combination with a yellow filter (Hoya, Los Angeles, CA, Y-46). The light-adapted bR had an absorbance of 0.6 at 570 nm in a 5 mm × 5 mm square cell. All spectra were obtained at room temperature, 25–27°C. Light adaptation was maintained during the course of the experiments, and any sample degradation, dark adaptation, or precipitation was below detection limits; i.e., there was no difference in either intensity or shape of the absorbance spectrum before and after the experiment. The rotational diffusion time was measured to be ~30 ms. The laser power was adjusted so that ~1% of the bR was photolyzed.

The LD instrumentation and the procedures for optical alignment were described previously (Che et al., 1994b). The polarizers were mounted on precision rotational stages that could be set with a resolution of 0.0025° and had extinction ratios of $\sim 1 \times 10^{-6}$. A Quanta RAY DCR-11 Nd:YAG laser, whose fundamental output was frequency doubled to 532 nm (repetition rate of 2 Hz), provided the photoselection-inducing excitation pulses. Neutral-density filters attenuated the laser power to 90 μJ per pulse (beam diameter ~9 mm). A 532-nm half-wave plate and a clean-up polarizer ensured the polarization purity of the excitation beam. The polarization of the laser defined the laboratory parallel direction. The transient LD of the bR sample was probed with a xenon flash lamp (beam diameter ~7 mm) whose power was such as to result in less than 0.25% photobleaching of the sample (Lewis et al., 1987) and whose beam traveled at 90° with respect to the laser beam propagation direction. The collimated beam passed through the polarizers and was focused into a Thermo Jarrell Ash Monospec 27 spectrograph with a 250-μm slit and a 150-groove/mm holographic grating blazed at 450 nm. The diffracted light was detected with an EG&G PAR1420 detector gated to 100 ns. A Stanford DG535 delay-pulse generator controlled the timing of the detector gate and the firing of the flash lamp with respect to the laser pulse. The time delay is defined as the time between the laser pulse and the center of the 100-ns gate of the gated detector. A polarizer rotation angle, β, of 2.5° was used. The probe polarizers were set to +45 and -45° with respect to the laser polarization. All polarizer positions and rotations were performed to within 0.01°.

The transient parallel absorption measurements used the same instrumentation as described above and shown in Fig. 2. The optical layout was essentially the same, except that the second polarizer, LP2, was removed and the polarization of LP1 was set parallel to the excitation pulse polarization. The laser power and polarization were exactly the same as in the LD measurements, and the measurements were conducted at the same delay times. Neutral-density filters were used to attenuate the probe beam intensity to be within the dynamic range of the detector.

TIME-RESOLVED PHOTOSELECTION-INDUCED LINEAR DICHROISM

The pseudo-null method is a sensitive tool to measure the time evolution of LD for biological molecules. However, care must be taken with LD measurements of chiral samples, for which CB contributes to the signal (Che et al., 1994b; Shapiro et al., 1995). For the data presented here, the photoinduced linear dichroism for the phototransformed bR sample is at least 1000 times greater than the CB signal. This is demonstrated in Fig. 3, which shows the ground-state spectrum (which in the absence of any photoselection or ground-state LD must contain only CB (Che et al., 1994b) compared with the photoinduced LD (t = 50 ns) spectrum.

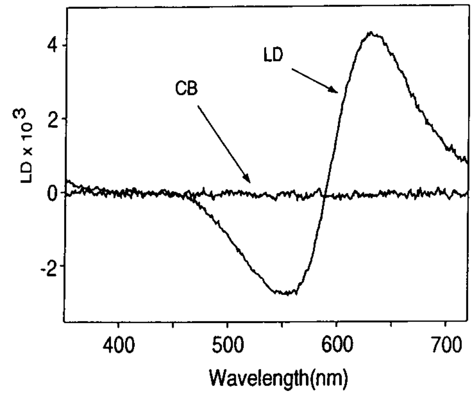

FIGURE 3 Comparison of the CB versus LD of bacteriorhodopsin. These are actual signals measured at the detector. The CB is the flat line, and the LD is the larger curve. The LD was taken 50 ns after excitation.

The all-*trans* chromophore of light-adapted bR and the 13-*cis* chromophores of the phototransformed bR are treated as linear absorbers within the spectral regions presented here. The absorbance of light at frequency ν with unit polarization U is

$$A_U(\nu) = \epsilon_U(\nu)CL, \quad (3)$$

where L is the path length, C is the molar concentration, and $\epsilon_U(\nu)$ is the decadic molar extinction coefficient that is proportional to $\mathbf{U} \cdot \boldsymbol{\mu}_{if}{}^2$, where $\boldsymbol{\mu}_{if}$ is the chromophore's transition dipole moment and $\mathbf{U}$ is a unit vector directed along the polarization direction. For optically thin samples, the change in absorbance is

$$\Delta A(t) = \log[I_o/I(t)], \quad (4)$$

where I_o and $I(t)$ are the transmitted intensities in the absence of an excitation pulse and at a time t after an excitation pulse, respectively.

The time-dependent LD is

$$\mathrm{LD}(t) = \Delta A_{\parallel}(t) - \Delta A_{\perp}(t), \quad (5)$$

and the dichroic ratio is defined as

$$\mathrm{d}(t) = \Delta A_{\parallel}(t)/\Delta A_{\perp}(t). \quad (6)$$

Photoselection on the isotropic membrane suspension

The orientational distribution of PM in aqueous suspension is isotropic. On irradiation with linearly polarized light, the bR proteins in the isotropic sample whose transition dipole moments are parallel with the polarization of the excitation pulse are preferentially excited (Albrecht, 1961). A probe beam can monitor the evolution of the photoselection-induced ordering as a function of time. Eventually, rotational diffusion will randomize the photoselection. For the sample presented here, however, the rotational diffusion time is orders of magnitude longer than the times analyzed here.

An ideal case of photoselection, which can be approached when the system is not in saturation, measures a dichroic ratio of 3 (Kliger et al., 1990). The theory of photoselection with intense laser pulses and saturation effects has been discussed in detail elsewhere (Magde, 1977; Nagle et al., 1983). However, in this experiment the low photolysis and a measured dichroic ratio of nearly 3 suggest that saturation can be neglected. A decrease in laser power decreased the LD signal without changing the measured dichroic ratio, which further indicates a lack of saturation.

ANISOTROPY AND ORIENTATIONAL DYNAMICS

After the bR suspension has been photoselected, the LD and the parallel absorption measurements can determine the reorientation of the transition dipole moment in the photolyzed population with respect to the unphotolyzed bR. After photoselection, the patches undergo thermal rotational diffusion. For the simplest case of a spherically symmetric solute with a single long-lived transition dipole moment, the time dependence of the LD is of the form

$$\mathrm{LD}(t) = \mathrm{LD}(0)\exp\left(\frac{-t}{6t_R}\right), \quad (7)$$

where $t_R = (\eta V)/kT$ is the isotropic rotational diffusion time constant, k is Boltzmann's constant, T is the absolute temperature, η is the viscosity, and V is the hydrodynamic volume for the solute (Michl and Thulstrup, 1986). It should be noted that the bR patch suspensions consist of many different-sized patches. Each patch has a different hydrodynamic volume and thus a different rotational diffusion time. The rotational diffusion time will be an average of the rotational diffusion times for the distribution of patch sizes. For the sample presented here, the ensemble average of the rotational diffusion constants is orders of magnitude larger (30 ms) than the times analyzed here. Therefore, the effect of rotational diffusion does not contribute to the time evolution of the anisotropy for the early K to early M intermediates.

For the bR photocycle presented in Fig. 1, the measured LD and parallel absorption are equal to the sum of the absorptions for each spectral intermediate present at the time of the measurement. If the system is far from saturation and the rotational diffusion is negligible, the parallel and perpendicular absorption difference and the LD after photoselection on the isotropic sample are (Che et al., 1994a; Otto et al., 1995)

$$\Delta A_{\parallel}(t,\lambda) = L\left[\left(\sum_i \epsilon_i(\lambda)K_i(t)(1 + 2\cos^2\theta_i)\right) - \epsilon_{bR}(\lambda)K_{bR}(t)(1 + 2\cos^2\theta_{bR})\right] \quad (8)$$

$$\Delta A_{\perp}(t,\lambda) = L\left[\left(\sum_i \epsilon_i(\lambda)K_i(t)(2-\cos^2\theta_i)\right) - \epsilon_{bR}(\lambda)K_{bR}(t)(2-\cos^2\theta_{bR})\right] \quad (9)$$

$$\mathrm{LD}(t,\lambda) = L\left[\left(\sum_i \epsilon_i(\lambda)K_i(t)(3\cos^2\theta_i-1)\right) - \epsilon_{bR}(\lambda)K_{bR}(t)(3\cos^2\theta_{bR}-1)\right] \quad (10)$$

where $\epsilon_i(\lambda)$ is the extinction coefficient at the probe wavelength, λ; the subscript i denotes the ith intermediate in the photocycle (of all species except the unconverted bR); $K_i(t)$ is a function that gives the concentration of each species at time t; L is the path length of the cell; θ_i is the angle between the transition dipole moment of the excitation transition and the transition dipole moment of the ith intermediate at time t; $K_{bR}(t)$ is the equivalent concentration of bR still in the photocycle, such that $\Sigma K_i(t) = K_{bR}(t)$ at any time t; and θ_{bR} is the angle between the excitation transition dipole moment and the probe transition dipole moment for bR, which is not necessarily the excitation transition (if more than one bR transition exists in a wavelength region, this term becomes a sum over those transitions). The ratio of the LD to the parallel absorption difference can be written as (11)

$$\frac{\mathrm{LD}(t,\lambda)}{\Delta A_{\parallel}(t,\lambda)} = \frac{\left[\left(\sum_i \epsilon_i(\lambda)K_i(t)(3\cos^2\theta_i-1)\right) - \epsilon_{bR}(\lambda)K_{bR}(t)(3\cos^2\theta_{bR}-1)\right]}{\left[\left(\sum_i \epsilon_i(\lambda)K_i(t)(1+2\cos^2\theta_i)\right) - \epsilon_{bR}(\lambda)K_{bR}(t)(1+2\cos^2\theta_{bR})\right]} = C(t,\lambda). \quad (11)$$

$C(t,\lambda)$ is functionally equivalent to the anisotropy, which is commonly defined as the ratio between the LD and the isotropic absorption difference. For the case that all the θ_{bR} and θ_i are zero, $C(t,\lambda)$ is 2/3 at all wavelengths, and there is no reorientation of the chromophore. As in Eqs. 8–10, the angle defined in Eq. 11 is the angle between the excitation transition dipole moment and the probe transition dipole moment, which includes all transitions of bR. Changes in this angle are considered reorientations. For each time and wavelength, the value of $C(t,\lambda)$ gives the ratio of the LD to the parallel absorption from the contributions of the intermediates that exist at time t (the following discussion of intermediates now includes the contribution of the bR bleaching band that corresponds to the subscript bR defined above). As the absorption approaches zero, Eq. 11 becomes singular, and it is satisfied by any choice of $C(t, \lambda)$. By determining $C(t, \lambda)$ experimentally it is possible to calculate the angle θ_i from Eq. 11 for each intermediate if both $K_i(t)$ and $\epsilon_i(\lambda)$ are known. This calculation requires only that these quantities be known at a specific time and wavelength for every intermediate that contributes to the signal at that time. Unfortunately, kinetic models for the bR photocycle are disputed, and the extinction values for each intermediate are unknown over a broad spectral range. These restrictions greatly complicate the exact determination of θ_i for the intermediates. There are, however, strategies to measure the time evolution of anisotropy across a broad spectral region that are model independent.

Because any change in anisotropy at a specific wavelength must result in changes in $C(t,\lambda)$, the wavelength dependence of $C(t,\lambda)$ would indicate which spectral transitions changed anisotropy. If $C(t,\lambda)$ is constant in time and in wavelength, then there is no observable rotation within the signal-to-noise ratio for the intermediates present, which absorb at the observed wavelengths during the time of observation. If there were reorientations, then $C(t,\lambda)$ could be constant in time and wavelength only if the extinctions of the intermediates contributing to the signal were indistinguishable or if a series of intermediates were to mimic the time- and wavelength-dependent absorption profile of another intermediate, or else the sums in Eq. 11 could not cancel at each wavelength. Such a series of complex cancellations may not be mathematically forbidden by Eq. 11 but is generally physically unrealistic. Any reorientations are seen as spectral features in the absorption band of the intermediate whose chromophore reorients. Conversely, the lack of spectral features precludes reorientations greater than the limits in sensitivity set by the signal-to-noise ratio.

This method of spectral decomposition has been presented in detail for steady-state transitions of oriented samples (Michl and Thulstrup, 1986; Thulstrup, 1980) and has been described for LD measurements on the photocycle of oriented bR samples in which anisotropy was the quantity measured at specific wavelengths (Otto et al., 1995).

If spectral features appear in regions of the spectrum where more than one spectral intermediate contributes, then both $K_i(t)$ and $\epsilon_i(\lambda)$ are needed to quantify the reorientation. Moreover, changes in spectral regions can be attributed to chromophore rotations of intermediates that absorb in the band where the spectral features appear. Over broad spectral ranges and for many times, spectrally distinct intermediates will exist. The larger the spectral range and differences in intermediates, the more isolated regions can be found. The ability to isolate specific spectral regions as a function of time makes the exact determination of $K_i(t)$ unnecessary. For example, for the broad bR (570 nm) bleaching band near the time of the major formation of M (410 nm), $C(t,\lambda)$ to the red of 570 nm would contain mostly contributions from bR. This would be true for any region with an intermediate that is spectrally distinct at a specific time.

In spectral regions where only one intermediate primarily contributes, Eq. 11 reduces to

$$\frac{\mathrm{LD}(t,\lambda)}{\Delta A_{\|}(t,\lambda)} = \frac{(3\cos^2\theta_{\mathrm{i}} - 1)}{(1 + 2\cos^2\theta_{\mathrm{i}})} = C_{\mathrm{i}}(t,\lambda), \qquad (12)$$

where

$$C_{\mathrm{i}}(t,\lambda) = 1 - \frac{1}{\mathrm{d}_{\mathrm{i}}(t,\lambda)}. \qquad (13)$$

This gives θ_{i} as

$$\theta_{\mathrm{i}}(\lambda) = \cos^{-1}\left[\frac{1 + C_{\mathrm{i}}(t,\lambda)}{3 - 2C_{\mathrm{i}}(t,\lambda)}\right]^{1/2}. \qquad (14)$$

θ_{i} can thus be determined from $C(t,\lambda)$ for each spectrally isolated intermediate at time t.

In spectral regions where more than one intermediate contributes, the sum in Eq. 11 must be expanded to include all those intermediates. If $C(t,\lambda)$ changes with time and wavelength then there are reorientations, and, as stated previously, both $K_{\mathrm{i}}(t)$ and $\epsilon_{\mathrm{i}}(\lambda)$ are needed to quantify each reorientation. But, if $C(t,\lambda)$ is constant, there can be no reorientation. Furthermore, if there is overlap between one intermediate and other intermediates that do not rotate and if there is no wavelength dependence on $C(t,\lambda)$, then that intermediate must not rotate. Obviously, the intermediate whose orientation is unknown must contribute substantially (above the noise level) to the signal at the wavelengths studied.

For broadband measurements, real data approach zero at some times and wavelengths. Consequently, the use of a ratio equation, such as Eq. 11, leads to singularities. For small signals, noise fluctuations compromise useful information that might be obtained from Eq. 10. In this case, in which data are obtained over a large spectral range and at many times, this computational difficulty may be pronounced and extend throughout a large portion of the spectrum for many times. To minimize this computational effect, it is more convenient to use the difference relation

$$\mathrm{LD}_{\mathrm{i}}(t,\lambda) - C_{\mathrm{i}}(t,\lambda)\Delta A_{\mathrm{i}\|}(t,\lambda) = 0, \qquad (15)$$

to determine $C(t,\lambda)$. Hence, in regions of the spectrum and at times for which the signal sizes are comparable with those of the noise, the calculated result is the difference in signal plus noise rather than the ratio of signal plus noise.

RESULTS AND DISCUSSION

LD and parallel absorption, $\Delta A_{\|}(t)$, were measured at 50 ns, 450 ns, 1 μs, 1.8 μs, 3.2 μs, 15 μs, and 50 μs following photolysis. Each time point is the average of 128 scans for the LD data and 4096 scans for the $\Delta A_{\|}(t)$ data. This demonstrates the improvement in the signal-to-noise ratio that the LD method offers. The raw data are shown in Figs. 4 and 5.

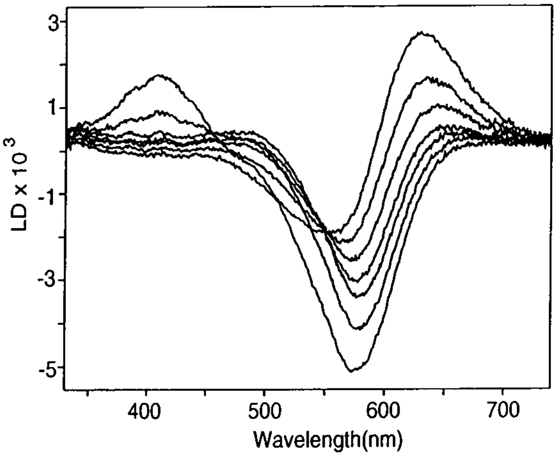

FIGURE 4 Measured LD spectra of bacteriorhodopsin at 50 ns, 450 ns, 1 μs, 1.8 μs, 3.2 μs, 15 μs, and 50 μs following excitation. The increasing magnitude of the absorption at 570 nm is the direction of increasing time. A polarizer rotation angle, β, of 2.5° was used.

In the analysis of the data, we determined $C(t,\lambda)$ by fitting Eq. 15 until the residuals (the left-hand side of Eq. 15 compared to zero) were minimized. A value of 0.67 for $C(t,\lambda)$ best satisfied Eq. 15. Fig. 6 shows residuals of Eq. 15 for different values of $C(t,\lambda)$. The selection of 0.67 as the most appropriate $C(t,\lambda)$ for the 50-ns time is supported by evaluation of the standard deviation (SD) of the left-hand side of Eq. 15 for the data as a function of wavelength. The SD for each value of $C(t,\lambda)$ is given in Table 1. In Fig. 6 there are definite spectral features for values less than 0.65 and minor differences between 0.66 and 0.67. Table 1 includes some larger values of $C(t,\lambda)$ to

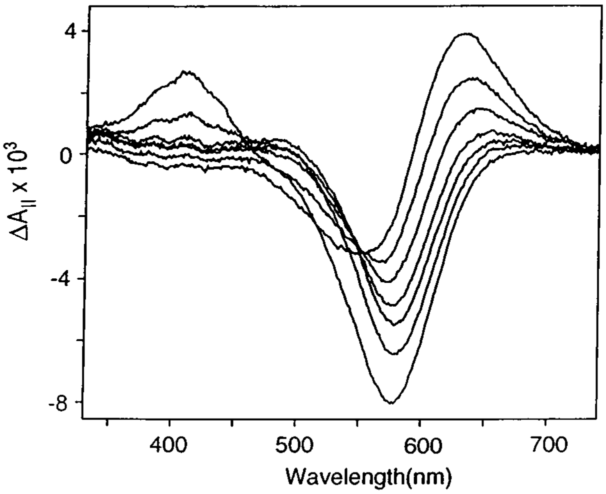

FIGURE 5 Measured $\Delta A_{\|}$ spectra of bacteriorhodopsin at 50 ns, 450 ns, 1 μs, 1.8 μs, 3.2 μs, 15 μs, and 50 μs following excitation. The increasing magnitude of the absorption at 570 nm is the direction of increasing time, as in Fig. 3.

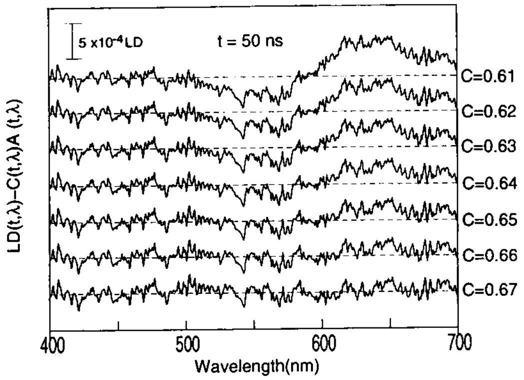

FIGURE 6 Left-hand side of Eq. 15 for the 50-ns time with different values of $C(t,\lambda)$. The appearance of spectral features becomes evident for values that differ from 0.67 by more than 0.01. The dashed lines indicate zero, and the curves are offset 5×10^{-4} optical density units. The scale is shown in the upper left-hand corner.

demonstrate that SDs of the residuals are reasonably symmetric near 0.67. Overall, we conclude by visual inspection and comparison of SDs that the best choice of $C(t,\lambda)$ to satisfy the left-hand side of Eq. 15 for all times and wavelengths examined is 0.67. The left-hand side of Eq. 15 with $C(t,\lambda)$ equal to 0.67 at all the times is shown in Fig. 7. The graph shows how well the left-hand side of Eq. 15 is satisfied (i.e., how well LD and $\Delta A_{\|}$ match in intensity and shape). There is no discernible difference in any of the graphs of Eq. 15 at the times shown for a constant $C(t,\lambda)$ value of 0.67. Inasmuch as it is only the angle dependence in Eq. 15 that can lead to changes in $C(t,\lambda)$ either spectrally or temporally, any reorientation would be seen as spectral features in the plots of the left-hand side of Eq. 15. Because no spectral features appear for any time within the signal-to-noise ratio for the experiment, there must be no reorientation within experimental sensitivity.

For most measurements, $C(t,\lambda)$ equal to 0.67 gave the minimum spectral features. There was a SD difference of the order of 10^{-6} between 0.67 and 0.66 at all times, whereas both these $C(t,\lambda)$ compared with smaller $C(t,\lambda)$ values gave differences in SD greater than 1×10^{-5} for all times. These variations could suggest that 1) the true value of $C(t,\lambda)$ lies somewhere between 0.66 and 0.67, 2) the noise in our measurements caused these variations to occur, or 3) there were reorientations that correspond to changes between 0.66 and 0.67. The signal-to-noise ratio in these measurements is insufficient to permit us to distinguish among these possibiities.

One can see the sensitivity for orientational motions in these measurements by noting how small a variation in $C(t,\lambda)$ results in an observable failure of Eq. 15. Fig. 6 and Table 1 give the variations for different $C(t,\lambda)$ values. Equation 14 gives

$$\delta\cos^2\theta = \left(5/(3-2C(t,\lambda))^2\right)\delta C(t,\lambda) \qquad (16)$$

TABLE 1 Determination of *C*(*t*, λ) and Sensitivity in θ° for the 50-ns time

$C(t,\lambda)$	Standard Deviation ($\times10^5$)	$\delta C(t,\lambda)$*	$\delta\theta°$*
0.70‡	12	0.03	n.a.
0.69‡	10	0.02	n.a.
0.68‡	9.0	0.01	n.a.
0.67	8.6	0	0
0.66	8.9	0.01	7.8
0.65	10	0.02	11
0.64	12	0.03	13
0.63	14	0.04	16
0.62	16	0.05	17
0.61	19	0.06	19

* For a true value of $C(t,\lambda) = 0.67$. Equation 16 can be used for other values.

‡ Mathematically significant but not physically meaningful.

Variations in $C(t,\lambda)$ larger than 0.01 caused the first distinguishable spectral features to appear, and, by Eq. 16, this corresponds to a variation in angle of ~8°. The visual appearance of the variations is shown in Fig. 6. Table 1 gives an indication of the size of angular variation for different variations in $C(t,\lambda)$ that correspond to the visual features in Fig. 6. Equation 16 and Eqs. 12–14 show that values of $C(t,\lambda)$ larger than 0.67 are nonphysical in regions where one intermediate primarily contributes, but mathematically the residuals for Eq. 15 should be symmetric around the best value of $C(t,\lambda)$. Because the data are over a large spectral range, 350–750 nm, and the value of $C(t,\lambda)$ required to satisfy Eq. 15 is independent of time and wavelength, this result is independent of any model. Because the signal at some specific wavelength region consists of mostly one intermediate, we should be able to detect any motions greater than these limits for that intermediate. This is definitely true for the bR band, which at early times contributes all the signal in the blue and at later times all the signal in

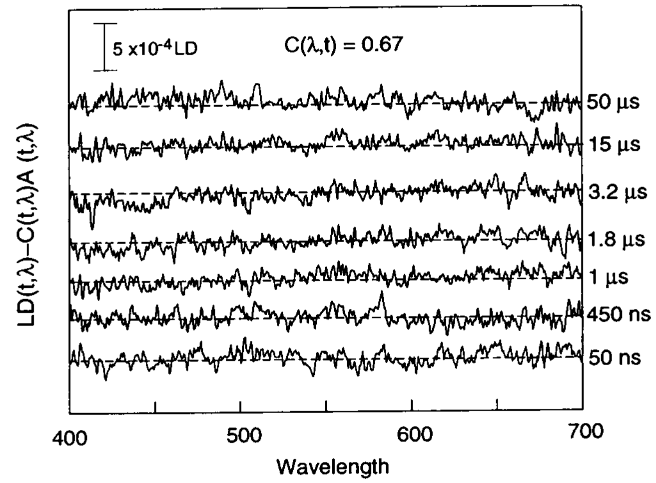

FIGURE 7 Left-hand side of Eq. 15 with a $C(t,\lambda)$ of 0.67 at 50 ns, 450 ns, 1 µs, 1.8 µs, 3.2 µs, 15 µs, and 50 µs. The dashed lines indicate zero, and the curves are offset 5×10^{-4} optical density units. The scale is shown in the upper left-hand corner.

the red. Hence, bR cannot rotate more than 8°. In regions where more than one spectral intermediate contributes, we can use the facts that the bR band does not rotate and that we observe no wavelength dependence of the anisotropy to determine the limit on the reorientation of the intermediates that contribute to this band. A model of the kinetics and extinction profiles of Lanyi and co-workers (e.g., Váró and Lanyi, 1991) predicts that, at the early times presented here, there will be overlap between L and bR. As we do not see any spectral features, we can say that L does not rotate more than 8°. Likewise, for the overlap among M, L, and bR at later times, the fact bR and L do not rotate, combined with the lack of a wavelength dependence on anisotropy, indicates that M cannot rotate more than the sensitivity limit of 8°.

Effects of sample conditions and preparation on the anisotropy

These results are inconsistent with other measurements of chromophore reorientation in PM suspensions for these intermediates (Wan et al., 1990, 1991; Song et. al., 1994). Those studies measured chromophore reorientations as large as 20°. Besides the technique used for measurements, there were some differences in sample conditions between our studies and the ones mentioned above. To see the effect of these differences, we collected data at sample conditions similar to those for previous studies (Song et al., 1994). The conditions that were varied were the buffer, the path length (and sample concentration), and whether the sample was flowed; all other experimental conditions were the same as described above. The data were analyzed as described above. The suspension buffer was changed to 10-mM phosphate buffer with 5-mM azide at pH 7.0. The experiment was repeated, and, with a $C(t,\lambda)$ of 0.67, no rotations were detected (data not shown). The sample was next placed in a 2-mm flow cell at 25°C in the above phosphate buffer. The sample's concentration was such that it had an absorbance of 0.7 at 568 nm. Unlike for the work by others (Song et al., 1994), when the sample was flowed at speeds greater than 4 mm/s a static LD signal (defined in Eq. 2) greater than 0.05 was detected. This signal was attributed to flow orientation; for the flow system used in this experiment the size of the signal was proportional to the flow rate. The flow orientation was reduced to an acceptable level (less than 0.01 signal unit) when the sample was flowed at less than 0.5 mm/s. The experiment described above was repeated under these new conditions and revealed, for a $C(t,\lambda)$ of 0.67, no detectable change in the anisotropy (data not shown). These data appeared similar to the data shown in Fig. 7, except for small differences in the signal sizes that were due to differences in concentration and photolysis. The conclusion is that differences in sample handling do not contribute to variations in measured anisotropy between laboratories.

Another possible explanation of the discrepancy involves differences in patch size. It was necessary that bR suspension be slightly sonicated, as described in Materials and Methods, to eliminate an unstable static signal in the bR absorption region. This signal varied between 0.01 to 0.05, as defined in Eq. 2, but disappeared after slight sonication. The static signal may be caused by gravitational orientation of large membrane patches or aggregates, which would preferentially orient with their membrane normal perpendicular to vertical. This makes the sample anisotropic and creates a static LD proportional to the gravitational orientation. The effect of light sonication would be to break up both aggregates and larger PM patches into smaller PM patches that are less susceptible to gravitational orientation. Gravitational orientation as a means to create anisotropy and the ability of sonication to reduce this type of orientation has been used in linear dichroism studies of DNA (Hiort et al., 1990).

Differences in average patch size among laboratories may explain the conflict in observed reorientation, independently of any orientational effects. One possible explanation may be that the curvature of the patches changes over the course of the photocycle; for large patches this curvature and its changes would be much more pronounced. Such curvature has been seen over the course of the photocycle by Czégé (1987) and possibly indirectly by Ahl and Cone (1984), who saw spectator rotations. Any rotation caused by either time-dependent patch curvature or "spectator" rotations would result in a change in anisotropy and would clearly be seen as time-dependent spectral features in the residuals of Eq. 15. Inasmuch as our data do not have these features, we conclude that spectator rotations cannot occur within the sensitivity limits of 8°. If spectral features had been observed as a result of spectator rotations, the sum in Eq. 11 would have needed to be expanded to include unphotolyzed bR to interpret them. Immobilized samples would be unlikely to exhibit curvature because of the rigidity of the sample. This explanation is by no means definitive but could point to a potentially revealing aspect of bR function. We also point out that patch curvature changes should be minimal at the low bleaches used in the photoselection experiments and therefore are unlikely to account for differences among experiments conducted at similar bleach levels.

CONCLUSION

We have explored the early-time intermediates of the bR cycle, but this broadband spectral technique, along with the method of analysis used to show lack of major reorientations, could also be applied to later photocycle intermediates. The loss of anisotropy as the result of rotational diffusion, however, must be accommodated in the analysis and interpretation. It would also be of interest to apply this technique to focus on specific intermediates in order to narrow the sensitivity below 8°. It should be emphasized that the $\cos^2\theta$ orientation due to photoselection limits the sensitivity and is insensitive to azimuthal motions around the excitation transition; polarization studies using photoselection on aqueous samples have inherent sensitivity limits. This technique could be applied to samples immobilized and oriented in gels to yield more precise determinations of the chromophore orientation of each intermediate.

The ultrasensitive LD technique used here greatly increases the signal-to-noise ratio of LD measurements and makes the detailed reorientation study of the bR chromophore in suspension presented here possible by including measurements over a large spectral range. This work shows that the bR chromophore's transition dipole moment rotates less than 8° with respect to the bR excitation transition.

We thank Dr. W. Stoeckenius for suggesting that a linear dichroism signal might arise from patch curvature changes. We especially thank Dr. M. P. Heyn for his helpful comments and discussions and Drs. R. A. Goldbeck, G. S. Harms, and C. K. Johnson for helpful discussions. R.M.E thanks the Patricia Harris Fellowship for support, and D.B.S thanks National Institutes of Health for support under NRSA 1F32HL08969. This work is supported by National Institutes of Health grants GM35158 to D.S.K. and GM43561 to R.A.B.

REFERENCES

Ahl, P. L., and R. A. Cone. 1984. Light activates rotations of bacteriorhodopsin in the purple membrane. *Biophys. J.* 45:1039–1049.

Albrecht, A. C. 1961. Polarizations and assignments of transitions: the method of photoselection. *J. Mol. Spectrosc.* 6:84–108.

Birge, R. R. 1990. Photophysics and molecular applications of the rhodopsins. *Annu. Rev. Phys. Chem.* 41:683–733.

Che, D., R. A. Goldbeck, and D. S. Kliger. 1994a. Theory of natural and circular dichroism in molecules orientated by *J. Chem. Phys.* 12: 8602–8613.

Che, D., D. B. Shapiro, R. M. Esquerra, and D. S. Kliger. 1994b. Ultrasensitive time-resolved linear dichroism spectral measurements using near-crossed linear polarizers. *Chem. Phys. Lett.* 224:145–154.

Czégé, J. 1987. Light-scattering changes during the photocycle of bacteriorhodopsin. *Acta Biochim. Biophys. Hung.* 22:463–478.

Czégé, J., and L. Reinisch. 1990. Cross-correlated photon scattering during the photocycle of bacteriorhodopsin. *Biophys. J.* 58:721–729.

Dencher, N. A., D. Dresselhaus, G. Zaccai, and G. Büldt. 1989. Structural changes in bacteriorhodopsin during the proton translocation revealed by neutron diffraction. *Proc. Natl. Acad. Sci. USA.* 86:7876–7879.

Han, B. G., J. Vonck, and R. Glaeser. 1994. The bacteriorhodopsin photocycle: direct structural study of two substrates of the M-intermediate. *Biophys. J.* 67:1179–1186.

Hauss, T., G. Büldt, M. P. Heyn, and N. A. Dencher. 1994. Light-induced isomerization causes an increase in the chromophore tilt in the M intermediate of bacteriorhodopsin: a neutron diffraction study. *Proc. Natl. Acad. Sci. USA.* 91:11854–11858.

Henderson, R. 1975. The structure of the purple membrane from *Halobacterium halobium*: analysis of the x-ray diffraction pattern. *J. Mol. Biol.* 93:123–138.

Heyn, M. P., R. J. Cherry, and U. Müller. 1977. Transient linear dichroism studies of bacteriorhodopsin: determination of the orientation of the 568-nm all-*trans* retinal chromophore. *J. Mol. Biol.* 121:607–620.

Heyn, M. P., and H. Otto. 1992. Photoselection and the transient linear dichroism with oriented immobilized purple membranes: evidence for motion of the C(20)-methyl group of the chromophore towards the cytoplasmic side of the membrane. *Photochem. Photobiol.* 56:6: 1105–1112.

Hiort, C., Bengt, N., and Rodger, A. 1990. Enantiopreferential DNA binding of $[\mathrm{Ru}^{\mathrm{II}}(1,10\text{-phenanthroline}]^{2+}$ studied with linear and circular dichroism. *J. Am. Chem. Soc.* 112:1971–1982.

Hwang, S. B., R. A. Bogomolni, Y. W. Tseng, and W. Stoeckenius. 1977. Angular orientation of an intermediate of the bacteriorhodopsin photochemical reaction cycle. *Biophys. J.* 17:98a.

Kliger, D. S., J. W. Lewis, and C. E. Randall. 1990. Polarized Light in Optics and Spectroscopy. Academic Press, New York.

Koch, M. H. J., N. A. Dencher, D. Oesterhelt, H-J. Plöhn, G. Rapp, and G. Büldt. 1991. Time-resolved x-ray diffraction study of structural changes associated with the photocycle of bacteriorhodopsin. *EMBO J.* 10: 521–526.

Lanyi, J. 1992. Proton transfer and energy coupling in the bacteriorhodopsin photocycle. *J. Bioenerg. Biomem.* 24:2:169–179.

Lewis, J. W., J. Warner, C. M. Einterz, and D. S. Kliger. 1987. Noise reduction in laser photolysis studies on photolabile samples using an optical multichannel analyzer. *Rev. Sci. Instrum.* 58:945–949.

Lozier, R. H., R. A. Bogomolni, and W. Stoeckenius. 1975. Bacteriorhodopsin: a light-driven pump in *Halbacterium halobium. Biophys. J.* 15:955–962.

Magde, D. Photoselection with intense laser pulses. 1977. *J. Chem. Phys.* 68:3717–3733.

Mathies, R. A., S. W. Lin. J. B. Ames, and W. T. Pollard. 1991. From femtoseconds to biology: mechanism of bacteriorhodopsin's light-driven proton pump. *Annu. Rev. Biophys. Chem.* 41:683–733.

Michl, J., and J. W. Thulstrup. 1986. Spectroscopy with Polarized Light: Solute Alignment by Photoselection and in Liquid Crystals, Polymers, and Membranes. VCH Publishers, New York.

Nagle, J. F., S. M. Bhattacharjee, L. A. Parodi, and R. H. Lozier. 1983. Effect of photoselection upon saturation and the dichroic ratio in flash experiments upon the effectively immobilized systems. *Photochem. Photobiol.* 38:331–339.

Oesterhelt, D., and W. Stoeckenius. 1971. Isolation of the cell membrane of *Halobacterium halobium* and its fractionation into red and purple membrane. *Meth. Enzymol.* 31:667–678.

Otto, H., and M. P. Heyn. 1991. Between the ground and M-state of bacteriorhodopsin the retinal transition dipole moment tilts out of the plane of the membrane by only 3°. *FEBS Lett.* 293:111–114.

Otto, H., C. Zscherp, B. Bourucki, and M. P. Heyn. 1995. Time-resolved polarized absorption spectroscopy with isotropically excited oriented purple membranes: the orientation of the electronic transition dipole moment of the chromophore in the O-intermediate of bacteriorhodopsin. *J. Phys. Chem.* 99:3847–3863.

Shapiro, D. B., R. A. Goldbeck, D. Che, R. M. Esquerra, S. J. Paquette, and D. S. Kliger. 1995. Nanosecond optical rotatory dispersion spectroscopy: application to the photolyzed hemoglobin-CO kinetics. *Biophys. J.* 68:326–334.

Song, Q., S. Harms, C. Z. Wan, and C. K. Johnson. 1994. Reorientations in the bacteriorhodopsin photocycle. *Biochemistry.* 33:14026–14033.

Stoeckenius, W., R. H. Lozier, and R. A. Bogomolni. 1979. Bacteriorhodopsin and the purple membrane of halobacteria. *Biochim. Biophys. Acta.* 505:215–278.

Subramaniam, S., M. Gerstein, D. Oesterhelt, and R. Henderson. 1993. Electron diffraction analysis of structural changes in the photocycle of bacteriorhodopsin. *EMBO J.* 12:1–8.

Thulstrup, E. W. 1980. Aspects of the Linear and Circular Dichrosim of Planar Organic Molecules. Springer-Verlag, New York.

Ulrich, A. S., I. Wallat, M. P. Heyn, and A. Watts. 1995. Reorientation of the retinal in the M-photointermediate of bacteriorhodopsin. *Nature Struct. Biol.* 2:190–192.

Váró, G., and J. K. Lanyi. 1991. Kinetic and spectroscopic evidence for an irreversible step between deprotonation and reprotonation of the Schiff base in the bacteriorhodopsin photocycle. *Biochemistry.* 5008–5015.

Wan, C., J. Qian, and C. K. Johnson. 1990. Time-resolved polarization study of anisotropy in bacteriorhodopsin. *J. Chem. Phys.* 94:8417–8423.

Wan, C., J. Qian, and C. K. Johnson. 1991. Conformational motion in bacteriorhodopsin: the K to L transition. *Biochemistry.* 30:394–400.

Wan, C., J. Qian, and C. K. Johnson. 1993. Light-induced reorientation in the purple membrane. *Biophys. J.* 65:927–938.